BMI-1 extends proliferative potential of human bronchial epithelial cells whilst retaining their mucociliary differentiation capacity.

Mustafa M. Munye[1]; Amelia Shoemark[2]; Robert A. Hirst[3]; Juliette M. Delhove[1]; Tyson V. Sharp[4]; Tristan R. McKay[5]; Christopher O'Callaghan[1]; Deborah L. Baines[6]; Steven J. Howe[1]; Stephen L. Hart[1]

AFFILIATIONS

[1] UCL Great Ormond Street Institute of Child Health, London, United Kingdom.

[2] Imperial College London, UK Electron Microscopy Dept, Royal Brompton and Harefield NHS Foundation Trust, London, UK.

[3] Primary Ciliary Dyskinesia Centre Department of Infection, Immunity and Inflammation, University of Leicester, Leicester, United Kingdom.

[4] Centre for Molecular Oncology, Barts Cancer Institute, Queen Mary University of London, London, United Kingdom.

[5] School of Healthcare Science, Manchester Metropolitan University, Manchester, United Kingdom.

[6] Institute for Infection and Immunity, St George's, University of London, London, United Kingdom

Correspondence should be addressed to M.M.M. (m.munye@ucl.ac.uk)

UCL Institute of Child Health, 30 Guilford Street, London, WC1N 1EH, United Kingdom

ABBREVIATIONS LIST

ALI = Air-Liquid Interface

BEGM = Bronchial Epithelial Growth Media

CBF = Cilia Beat Frequency

CFBE = Cystic Fibrosis Bronchial Epithelial

CRCs = Conditionally Reprogrammed Cells

DMEM = Dulbecco's Modified Eagle Medium

GFP = Green Fluorescent Protein

HBE = Human Bronchial Epithelial

hESCs = human Embryonic Stem Cells

hTERT = human Telomerase Reverse Transcriptase

iPSCs = induced Pluripotent Stem Cells

I_{sc} = short circuit current

NHBE = Normal Human Bronchial Epithelial

ODA = Outer Dynein Arms

PBS = Phosphate Buffered Saline

PCD = Primary Ciliary Dyskinesia

ROCK = Rho-associated protein kinase

ABSTRACT

Air-liquid interface (ALI) culture of primary airway epithelial cells enables mucociliary differentiation providing an *in vitro* model of the human airway but their proliferative potential is limited. To extend proliferation, these cells were previously transduced with viral oncogenes or mouse *Bmi-1* + *hTERT* but the resultant cell lines did not undergo mucociliary differentiation. We hypothesised that use of human *BMI-1* alone would increase the proliferative potential of bronchial epithelial cells while retaining their mucociliary differentiation potential. CF and non-CF bronchial epithelial cells were transduced by lentivirus with *BMI-1* then their morphology, replication kinetics and karyotype were assessed. When differentiated at ALI, mucin production, ciliary function and transepithelial electrophysiology were measured. Finally, shRNA knockdown of *DNAH5* in BMI-1 cells was used to model primary ciliary dyskinesia (PCD). BMI-1 transduced basal cells showed normal cell morphology, karyotype and doubling times despite extensive passaging. The cell lines underwent mucociliary differentiation when cultured at ALI with abundant ciliation and production of the gel-forming mucins MUC5AC and MUC5B evident. Cilia displayed a normal beat frequency and 9+2 ultrastructure. Electrophysiological characteristics of BMI-1 transduced cells were similar to un-transduced cells. shRNA knockdown of *DNAH5* in BMI-1 cells produced immotile cilia and absence of DNAH5 in the ciliary axoneme as seen in cells from patients with PCD. BMI-1 delayed senescence in bronchial epithelial cells, increasing their proliferative potential but maintaining mucociliary differentiation at ALI. We have shown these cells are amenable to genetic manipulation and can be used to produce novel disease models for research and dissemination.

65 Key words: air-liquid interface, airway model, lung, mucociliary differentiation,
66 primary ciliary dyskinesia

INTRODUCTION

The ciliated epithelium lining the airways provides the first line of defence to inhaled pathogens and particles and plays a crucial role in many respiratory diseases. It is possible to remove respiratory epithelial cells from the nose or upper airways of donors by brushing and culture them in the laboratory on collagen-coated, semi-permeable membranes. The progenitor basal epithelial cells from the brushings cultured at Air-Liquid Interface (ALI) differentiate into a fully ciliated, pseudostratified epithelium closely resembling that found in the airway (3).

If cells are obtained from a donor with a lung disease, e.g., cystic fibrosis, primary ciliary dyskinesia (PCD), asthma and chronic obstructive pulmonary disease, these ALI cultures provide a surrogate model of the diseased lung for research into pathogenic mechanisms and for the development of new therapeutics(9, 14, 16). However, basal epithelial cells can only be passaged 2-3 times before they lose their proliferation and differentiation potential (6, 18). Thus, to establish the wider use of basal cells in ALI epithelial culture models, methods are required that enable basal cells to be cultured for longer, genetically engineered, expanded and stored easily prior to differentiation on ALI cultures. Such cells would also overcome ethical issues related to repeated brushing of volunteers.

Recent approaches to extend the utility of primary, basal epithelial cells involved culturing them with rho-associated protein kinase (ROCK) inhibitors on a layer of irradiated feeder cells to provide cell-derived growth factors (18, 27). The requirement for irradiated feeder cells makes the maintenance of basal cell cultures complex and time-consuming, difficult to scale up and may limit the use of this approach to specialist laboratories. Alternatively, induced pluripotent stem cells (iPSCs) and embryonic stem cells (hESCs) were differentiated into mature respiratory epithelial cells and used to generate a pseudostratified epithelium expressing CFTR (30). However, the process takes several weeks and often the resulting cultures are not suitable for disease modelling as they are contaminated with endodermal

cell types (31) and often present with karyotypic anomalies which may confound drug screening efforts.

Extended proliferative potential of primary human bronchial epithelial (HBE) cells was described by transduction of basal cells with the mouse polycomb complex protein *Bmi-1* and human telomerase reverse transcriptase (*hTERT*) (6). Unlike cells transformed with viral oncogenes, *Bmi-1+hTERT* cell lines had no chromosomal abnormalities and produced a pseudostratified epithelium on ALI but gave only sparse ciliogenesis. This limited differentiation capacity may be explained by reports that *hTERT*, following long-term growth in culture, up-regulates expression of the potent mitogen c-Myc, so promoting entry into the cell cycle (21) thereby impeding ciliogenesis.

We hypothesised that BMI-1 transduction alone may overcome these issues observed with *Bmi-1+hTERT*, to produce basal cells with the potential for extended proliferation that retain their differentiation capacity on ALI. In this study, *BMI-1* transduced primary basal epithelial cells from CF and healthy donors were investigated for their morphology, growth characteristics and karyotype. We also assessed the cells mucociliary differentiation potential at ALI along with their Na^+ and Cl^- transport properties in Ussing chamber studies. We then demonstrate their use for the production of novel engineered disease models by shRNA knockdown of *DNAH5*, a gene associated with PCD, a ciliopathy with significant lung pathology resulting from abnormal mucociliary clearance. *BMI-1* transduction offers a facile method to greatly extend the utility of basal epithelial cells for translational and basic research.

MATERIALS & METHODS

Materials

Primary antibodies used in this study can be found in Table 1. Secondary antibodies for immunofluorescence were anti-IgG antibodies conjugated with AlexaFluor dyes (Invitrogen, Life Technologies). Secondary antibodies for Western blots were horseradish peroxidase-conjugated (HRP-conjugated) anti-IgG antibodies (Dako, Agilent Technologies).

Collagen Coating

Tissue culture flasks and transwells were coated for 1 hour at room temperature with 1% (v/v) solution of a 3mg/mL bovine collagen solution (PureCol; Advanced Biomatrix) in phosphate buffered saline (PBS), then washed with distilled water and air-dried.

Cell Culture

HEK293T cells were cultured in Dulbecco's Modified Eagle Medium (DMEM) supplemented with 10% (v/v) foetal bovine serum. Normal human bronchial epithelial (NHBE) cells, cystic fibrosis human bronchial epithelial cells (CFBE) cells were grown on collagen-coated plastic in bronchial epithelial growth media (BEGM; Lonza). All cells were grown at 37^{o}C and 5% CO_2. NHBE and CFBE cells were purchased from Lonza and Epithelix SàRL.

Lentivirus Production and Transduction

Full-length human BMI-1 cDNA was PCR cloned from pHR-EF1α-BMI1-IRES-GFP plasmid(20) with *XhoI* and *BamHI* sites added and TOPO cloned into pCR4 TOPO vector before being subcloned into pLVX-Puro vector digested with *XhoI* and *BamHI*. Lentivirus was produced as previously described(20), concentrated by centrifugation

at 4,500 x g for 18 hours at 4°C, re-suspended in OptiMem and added to cell media to transduce NHBE and CFBE cells (Lonza) at passage 2.

Doubling Time Analysis

NHBE and NHBE BMI-1 cells at varying passage numbers were seeded at densities of 30,000 cells per well onto collagen-coated 12-well plates. Cells were detached using trypsin-EDTA following 1-4 days in culture and total cell numbers per well were counted using a haemocytometer. An online calculator was used to calculate the doubling time (Roth V. 2006 Doubling Time Computing, Available from: http://www.doubling-time.com/compute.php). Doubling times were calculated using the formula;

$$doubling\ time = \frac{duration \times \log(2)}{\log(final\ cell\ count) - \log(initial\ cell\ count)}$$

Where cell count values were mean cell count of 3 independent wells.

Western Blotting

Cells were lysed with Cell Extraction Buffer (Life Technologies), boiled in the presence of NuPage LDS Sample Buffer (Life Technologies) and loaded onto NuPage Novex 4-12% Bis-Tris gels (Life Technologies). Electrophoresis and protein transfer onto Immobilon-P polyvinylidene fluoride membranes were performed using standard protocols. Antibodies against BMI-1, p16Ink4a and GAPDH and appropriate HRP-conjugated secondary antibodies were used for probing with bands visualised using Pierce ECL Western Blotting Substrate (Life Technologies, Paisley, UK) and a UVIchemi chemiluminescence imaging system (UVItec).

Air-liquid Interface (ALI) Culture

Cells grown to ~80% confluence in T75 flasks were trypsinised, seeded at a density of 900,000 cells/cm^2 on Transwell inserts (Corning) and grown at an ALI as previously described(8). Cell were maintained at an ALI for 4 weeks before analyses were performed.

Quantitative Reverse Transcription PCR (qRT-PCR)

Unless indicated, all reagents for qRT-PCR were obtained from ThermoFisher. Total RNA was harvested from cells using RNeasy Mini Kit (Qiagen) and potential DNA impurities digested using DNase I enzyme (TURBO DNA-free kit). Purified RNA was reverse transcribed with 2.5U/µL murine leukaemia virus (MuLV) reverse transcriptase at 42^{o}C for 1 hour in a reaction containing 1x GeneAmp PCR Gold Buffer, 1mM each dNTP, 5µM random hexamers, 5mM $MgCl_2$ and 1U/µL RNase inhibitor. The resulting cDNA was used in a qPCR reaction containing 1x Platinum Quantitative PCR SuperMix-UDG w/ROX and 1x TaqMan Gene Expression Assay primer/probe set (GAPDH primer/probe set Hs99999905_m1; DNAH5 primer/probe set Hs00292485_m1). The PCR reaction cycles used were 50^{o}C for 2 minutes, 95^{o}C for 10 minutes, 40 cycles of 95^{o}C for 15 seconds and 60^{o}C for 1 minute on an ABI PRISM 7000 Sequence Detection System (Applied Biosystems). Fluorescence data was collected at the end of each 60^{o}C reaction and relative expression levels calculated using the delta-delta Ct (2- ΔΔCt) method(19).

Immunofluorescence Staining and Confocal Microscopy

Cells were fixed with 4% PFA for 10 minutes at room temperature, washed with PBS and permeabilised with PBS-Triton (PBS 0.1% (v/v) Triton-X100) for 10 minutes at room temperature before blocking, immunostaining and mounting on microscope slides as previously described(26). Images were obtained using an Inverted Zeiss

LSM 710 Confocal microscope with the appropriate excitation lasers selected for the dyes used.

Fluorescence Microscopy

Bright-field and fluorescence images were captured with a Nikon Digital Sight DS-QiMC video camera attached to a Nikon Eclipse Ti-U inverted microscope. Videos and images were processed using NIS Elements AR software (Nikon, v4.00.12).

TEM for Cilia Ultrastructure

Ciliated cells cultured at an ALI were scraped and cells washed off with 200µL warmed BEBM. Cells were fixed by addition of 2mL of 2.5% glutaraldehyde and stored at 4^{o}C for at least 24 hours prior to further processing as previously described(24). Assessment of cilia ultrastructure was undertaken blinded by Dr Amelia Shoemark, a member of the PCD diagnostic service team at the Royal Brompton & Harefield NHS Foundation Trust, UK.

High-Speed Video Microscopy

High-speed video was recorded using a MotionPro X4 high-speed motion camera attached to a Nikon Eclipse Ti-U inverted microscope built with an environmental chamber. Videos were recorded at a frame rate of 500fps using Motion Studio software (IDT Vision, v2.11) with cells maintained at 37^{o}C.

For cilia beat frequency (CBF) assessment, ALI cultures were washed twice with PBS to remove mucus that may have affected CBF. After washing, the cells were allowed to equilibrate at 37^{o}C and 5% CO_2 for 20 minutes before video recording. At least four independent cultures per donor line were videoed with five areas recorded per culture, i.e., at least 20 videos were captured per donor line. To minimise bias

videos were recorded from the top, bottom, left, right and centre region of each culture and cilia beat-frequency assessed using CiliaFA software(25).

Electrophysiology Studies

Cells were grown at ALI for 4 weeks on Snapwell membranes (Corning) to enable mucociliary differentiation. Snapwells were then mounted on Ussing chambers and short circuit current (Isc) was measured as previously described (32). Briefly, monolayers were mounted in Ussing chambers in physiological salt solution consisting of 117mM NaCl, 25mM NaHCO3, 4.7mM KCl, 1.2mM MgSO4, 1.2mM KH2PO4, 2.5mM CaCl2 and 11mM d-glucose. The solution was continuously circulated throughout the course of the experiment and maintained at 37^{o}C whilst bubbled with 21% O_2 + 5% CO_2 premixed gas. Monolayers were first maintained under open-circuit conditions until transepithelial potential difference (V_t) and resistance stabilised. The cells were then short-circuited by clamping V_t at 0 mV using a DVC-4000 voltage/current clamp, and Isc was measured and recorded using a PowerLab computer interface. Every 30 seconds the preparations were returned to open-circuit conditions for 3 seconds so that the spontaneous V_t could be measured and trans-epithelial electrical resistance (TEER) calculated. Drugs were circulated in physiological salt solution and added in the order of amiloride (10 μM, apical), forskolin (25 μM, apical and basolateral) and GlyH-101 (10 μM, apical).

RESULTS

Characterisation of BMI-1 transduced cells in submerged culture

Primary NHBE cells maintained in submerged cultures displayed a characteristic cobblestone appearance (Figure 1a) but by passage 3 cells became elongated in appearance (white arrow; Figure 1b) and squamous differentiation was evident (black arrow; Figure1b). In contrast, BMI-1 transduced NHBE cells (NHBE-BMI-1) maintained their cobblestone appearance following extensive passaging, for example at passage 11 (Figure 1c) and passage 17 (Figure1d). However, squamous cells became evident following 25 passages (Figure 1e) after which the cells senesced, with no observable cell division for ten days. The cells maintained a normal diploid karyotype even at passage 23 (Figure 2).

BMI-1 down-regulates expression of the pro-senescent protein p16Ink4A. NHBE cells transduced with BMI-1 had low levels of p16Ink4A protein and high levels of BMI-1 (Figure 3a). Levels of BMI-1 in untransduced NHBE cells declined with an increase in passaging whilst levels of p16Ink4A increased and were higher in senesced, untransduced NHBE cells at passage 6 while BMI-1 expression was not evident by Western blot (Figure 3a).

SV40 large T-antigen or ROCK inhibition extends the replication potential of basal cells but alters the proliferation rate of the cells(4, 7, 12) therefore we assessed the doubling times of BMI-1 transduced cells at different passages (Figure 3b). We determined that untransduced cells at passage 2 had a doubling time of 1.18 days similar to BMI-1 transduced cells at passages 12 and 15 (doubling times of 1.25 and 1.21 days respectively) although by passage 23 the doubling time had increased to 1.49 days, consistent with observations of senescence at passage 25.

Differentiation of NHBE-BMI-1 Cells

NHBE-BMI-1 basal cells were subsequently analysed for their differentiation potential when cultured at ALI. After 2 -3 weeks culture, both primary NHBE and NHBE-BMI-1 cells produced motile cilia (Video 1a and b respectively). NHBE-BMI-1 cells maintained the ability to differentiate and produce cilia even at passage 15.

To quantify cilia function, we assessed cilia beat frequency of both primary and BMI-1 transduced NHBE and CFBE cells. Beating cilia from CFBE cells could not be detected, most likely due to the build-up of viscous mucus hindering cilia beating, until cultures were washed. As such, CFBE and NHBE cultures were washed twice prior to video recording and CBF analysis as detailed in the methods section.

CBF analysis of both primary and BMI-1 transduced NHBE and CFBE cells showed mean values within the normal range for respiratory cilia of 9-17Hz(25) (Figure 4a and b). Primary NHBE and NHBE-BMI-1 cells had a CBF of 16.7±0.2Hz and 15.3±0.2Hz respectively (Figure 4a) and primary CFBE and CFBE-BMI-1 cells exhibited CBF values of 12.9±0.3Hz and 14.3±0.3Hz respectively.

Further evidence of differentiation was demonstrated by immuno-detection, in NHBE-BMI-1 cells, of the tight junction protein occludin (Figure3c) and the mucins MUC5AC and MUC5B (Figure 4d, e). In addition, basal cells were present and indicated by p63 staining (Figure 4f) and BMI-1 protein was present in all nuclei (Figure 4g). The ciliary protein acetylated α-tubulin was also detected by immunostaining and highlighted abundant ciliation (Figure 4h). Further analysis of the cilia in differentiated NHBE-BMI-1 cells by TEM showed that they had a normal 9+2 ultrastructure with both inner and outer dynein arms present (Figure 4i, Table 2 and Table 3).

Electrophysiology studies

Primary HBE cells grown on ALI develop a trans-epithelial electrical resistance (TEER) with ion transport properties that can be measured by mounting of cultured epithelia on Ussing chambers and addition of drugs that can activate or inhibit specific cell surface ion channels. Cultures of primary NHBE cells from two different donors showed baseline TEER values of 331.1±105.5Ω.cm^2 and 621.0±33.2Ω.cm^2 (Table 4) and primary CFBE cells developed TEER of 1307.9±36.6Ω.cm^2. Similarly, *BMI-1* transduced NHBE and CFBE cells developed high TEER when grown at an ALI (1268.4±78.4Ω.cm^2 and 917.6±165.3Ω.cm^2 respectively; Table 4) demonstrating the cells retained their ability to form an electrically resistive epithelium.

Short circuit current (I_{sc}) analysis in Ussing chambers of NHBE and CFBE cells revealed that both primary NHBE cells and passage 13 NHBE-BM-1 cells cultured at ALI also had similar electrophysiology. Amiloride (10μM), an inhibitor of the epithelial Na^+ channel ENaC reduced I_{sc} in all cultures, although the amiloride-sensitive I_{sc} was variable. Subsequent elevation of cellular cAMP with forskolin (25μM) increased I_{sc} and this elevation was inhibited by the CFTR inhibitor Gly-H101 (10μM) (Figure 5 a, b). Thus, ENaC and CFTR-mediated ion transport was retained in NHBE-BMI-1 cells. Primary CFBE cells and passage 17 CFBE BMI-1 cells cultured at ALI also exhibited amiloride-inhibitable I_{sc} but no response to either forskolin or GlyH-101 was observed, as expected due to the lack of CFTR in these cells (Figure 5 c, d). Thus, CFBE-BMI-1 cells, like NHBE-BMI-1, also maintain the Na+ and Cl- ion transport characteristics of non-transduced primary CF cells.

Use of BMI-1 transduced cells to generate PCD cell models

We next explored the potential use of the BMI-1 transduced NHBE cells to generate an in vitro model of PCD. The outer dynein arm protein *DNAH5* is the most commonly mutated gene but even so this is a rare disease and cells are often not readily available. Cells with *DNAH5* mutations lack the DNAH5 protein in the ciliary axoneme and have missing outer dynein arms (ODAs) (13). NHBE cells transduced with BMI-1 were additionally transduced with a DNAH5 shRNA lentiviral construct that also expresses green fluorescent protein (GFP).

DNAH5 expression in shRNA-transduced cells was silenced by approximately 75% relative to untransduced cells (Figure 6a) while scrambled shRNA had no effect on *DNAH5* expression indicating silencing specificity.

NHBE-BMI-1 cells transduced with the two shRNAs were subsequently cultured at ALI to promote differentiation and ciliation. Following mucociliary differentiation, NHBE-BMI-1 GFP-positive cells, transduced with scrambled shRNA had motile cilia, (Video 2a) whereas GFP-positive *DNAH5* shRNA silenced cells had immotile cilia (Video 2b). However, in GFP negative cells (and by extension also *DNAH5* shRNA negative) motile cilia were still observed (Video 2c).

In untransduced NHBE BMI-1 cells and those GFP-positive cells transduced with the scrambled shRNA, DNAH5 was localised to the ciliary axoneme in all ciliated cells assessed as shown by co-localisation with acetylated α-tubulin expression. In contrast, in DNAH5 shRNA transduced GFP-positive cells, only 2.9% (5/173) of ciliated cells had DNAH5 in the ciliary axoneme (Figure 6b and Table 5).

DISCUSSION

Airway diseases are a significant cause of morbidity and mortality. Mucociliary differentiation of primary airway epithelial cells using ALI culture methods provides an *in vitro* model that faithfully recapitulates the *in vivo* airway epithelium for the study of disease pathology and therapies. However, these cells can only be cultured for 2-3 passages before they lose their ability to differentiate(5). This has important practical, ethical and cost implications for research in the field. Traditional cell transformation methods, using viral oncogenes that promote entry into the cell cycle, produce immortal cell lines incapable of mucociliary differentiation most likely due to their inability to suspend cell division and allow cilia production and differentiation.

We have shown that prevention of cellular senescence by expression of *BMI-1* allows extended passaging of HBE cells from CF and non-CF donors. Western blot analysis highlighted that senescent primary NHBE cells had accumulated high levels of the pro-senescent protein $p16^{Ink4a}$ in agreement with other studies (1, 6, 20). *BMI-1* transduced cells, however, showed low levels of $p16^{Ink4a}$ thereby delaying cell senescence as reported previously(15).

In addition to exhibiting delayed senescence, *BMI-1* transduced cells retained their cell phenotype, karyotype, ion transport characteristics and mucociliary differentiation potential with abundant ciliation observed when cultured at ALI. Ussing chamber studies revealed that, like primary HBE cells, *BMI-1* transduced NHBE and CFBE cells formed electrically resistive cultures and the direction of change in I_{sc} was as expected upon addition of amiloride, forskolin and the CFTR inhibitor Gly-H101. We note that baseline TEER values varied between HBE donors as did the magnitude of change in I_{sc} upon addition of amiloride, forskolin and the CFTR

inhibitor Gly-H101. Such variation has also been observed by Tosoni et al. (29) who recently demonstrated baseline TEER values ranged from 309 to 2963Ω.cm^2 in ALI cultures generated from the cells of 18 healthy donors.

In agreement with our findings, Torr et al(28) recently demonstrated that transduction of basal cells, from different two donors, with human *BMI-1* alone extends the proliferative potential of NHBE cells whilst retaining their differentiation potential as demonstrated by immunostaining and scanning electron microscopy. Our study extends on these findings demonstrating that passaging capacity of diseased cells (CFBE) can also be extended using this method. Taken together this would suggest *BMI-1* transduction of bronchial epithelial cells permits extended passaging and mucociliary differentiation independent of donor and/or disease status although further studies are needed to confirm this.

BMI-1 transduction did not immortalise the HBE cells in contrast to viral antigens such as the SV40 large T-antigen used to produce the 16HBE14o- cell line(5). However, *BMI* transduced cells could still be differentiated at 20-25 passages representing a significant advantage of this method over use of viral antigens. Using the ALI culture protocol outlined in the current study one can routinely obtain from 6-8 functional epithelial transwells in a 24-well ALI culture format per passage enabling the generation of a minimum of ~90-100 transwells from a single donor. This is significantly higher than the 10-15 epithelial transwells that can be generated with ~1x10^6 primary bronchial epithelial cells (typical quantity obtained from commercial providers) or brushing of the nasal turbinate of a single donor(29). Furthermore, sub-culturing of *BMI-1* transformed cells, as opposed to seeding ALI cultures, would enable banking of early passage cells and the potential to generate exponentially more functional epithelia at each passage.

Tosoni et al. (29) recently demonstrated that ALI cultures generated from different healthy donors can yield epithelia with vastly different physiological properties and drug responses. The *BMI-1* transduction protocol enables the generation of a large number of epithelia generated from donors with similar genetic backgrounds, or indeed from a single donor, allowing the study of disease pathophysiology in a manner that avoids the influence of genetic variability in cells from different donors. This highlights the potential for the development of personalised treatments using BMI-1 transduced cells.

In addition, an extended passaging capacity affords the opportunity for modification of HBE cells to create new models, to better understand disease and find novel treatments. As a proof of concept, we transduced NHBE BMI-1 cells with shRNA targeted against *DNAH5* in an attempt to create a model of PCD. The shRNA construct contained a GFP reporter to allow for selection of cells in which the *DNAH5* shRNA was expressed. Focussing on cells expressing GFP, we demonstrated loss of ciliary motility and absence of DNAH5 in the ciliary axoneme of cells transduced with the *DNAH5* targeted shRNA so mimicking the phenotype seen in patient cells(13). shRNA-mediated knockdown has been previously used to model PCD in otherwise healthy primary HBE cells (10, 11, 17) but these cells were not long lived so could not be used for further study to assess, for example, protein interactions or novel treatments. Gene addition, shRNA knockdown, or genome editing of BMI-1 transduced HBE cells could therefore provide a more useful tool for the study of a number of airway diseases.

Recently the use of pharmacological Rho-kinase inhibition along with co-culture of HBE cells with irradiated feeder-layer fibroblasts has been described to allow indefinite passage of HBE cells whilst retaining the cells differentiation capacity when

placed at ALI (18, 27). However, studies where the mucociliary differentiation potential of CRCs have been assessed have not reported successful mucociliary differentiation beyond passage 11(2, 22, 27). Furthermore, CRC morphology and doubling times differ significantly to their parent cells with CRC cells being smaller and growing in colonies as well as showing faster proliferation rates(18, 27). Following viral transduction, *BMI-1* expressing NHBE and CFBE cells are cultured exactly as non-transformed primary cells, without the need for a feeder layer, a factor that is likely to aid in the rapid uptake of this method of transformation and dissemination of the resulting cell models between laboratories and in the maintenance of cells in biobanks.

In summary, here we have shown that *BMI-1* transduction delays senescence in HBE cells from healthy and CF donors whilst maintaining the cells mucociliary differentiation potential. We have undertaken extensive characterisation of the differentiated cells showing normal ciliary beat frequency and ciliary ultrastructure. Ussing chamber studies with BMI-1 transformed NHBE and CFBE cells showed that these cells exhibit similar Na+ and Cl- ion transport characteristics to their respective primary cells, validating their use as models of CF. Furthermore, we have demonstrated how BMI-1- transduced cells can be engineered by further transduction with DNAH5 shRNA to recapitulate an in vitro disease model of primary ciliary dyskinesia, a valuable feature when studying rare diseases such as PCD where patient samples are difficult to obtain.

REFERENCES

1. **Brookes S, Rowe J, Gutierrez Del Arroyo A, Bond J, and Peters G**. Contribution of p16(INK4a) to replicative senescence of human fibroblasts. *Exp Cell Res* 298: 549-559, 2004.
2. **Butler CR, Hynds RE, Gowers KH, Lee Ddo H, Brown JM, Crowley C, Teixeira VH, Smith CM, Urbani L, Hamilton NJ, Thakrar RM, Booth HL, Birchall MA, De Coppi P, Giangreco A, O'Callaghan C, and Janes SM**. Rapid Expansion of Human Epithelial Stem Cells Suitable for Airway Tissue Engineering. *Am J Respir Crit Care Med* 194: 156-168, 2016.
3. **Chu Q, Tousignant JD, Fang S, Jiang C, Chen LH, Cheng SH, Scheule RK, and Eastman SJ**. Binding and uptake of cationic lipid:pDNA complexes by polarized airway epithelial cells. *Hum Gene Ther* 10: 25-36., 1999.
4. **Cozens AL, Yezzi MJ, Kunzelmann K, Ohrui T, Chin L, Eng K, Finkbeiner WE, Widdicombe JH, and Gruenert DC**. CFTR expression and chloride secretion in polarized immortal human bronchial epithelial cells. *Am J Respir Cell Mol Biol* 10: 38-47, 1994.
5. **Cozens AL, Yezzi MJ, Kunzelmann K, Ohrui T, Chin L, Eng K, Finkbeiner WE, Widdicombe JH, and Gruenert DC**. CFTR Expression and Chloride Secretion in Polarized Immortal Human Bronchial Epithelial Cells. *Am J Respir Cell Mol Biol* 10: 38-47, 1994.
6. **Fulcher ML, Gabriel SE, Olsen JC, Tatreau JR, Gentzsch M, Livanos E, Saavedra MT, Salmon P, and Randell SH**. Novel human bronchial epithelial cell lines for cystic fibrosis research. *Am J Physiol Lung Cell Mol Physiol* 296: 82-91, 2009.
7. **Fulcher ML, Gabriel SE, Olsen JC, Tatreau JR, Gentzsch M, Livanos E, Saavedra MT, Salmon P, and Randell SH**. Novel human bronchial epithelial cell lines for cystic fibrosis research. *Am J Physiol Lung Cell Mol Physiol* 296: L82-91, 2009.
8. **Hirst RA, Rutman A, Williams G, and Callaghan CO**. Ciliated Air-Liquid Cultures as an Aid to Diagnostic Testing of Primary Ciliary Dyskinesia. *Chest* 138: 1441-1447, 2010.
9. **Hirst RA, Rutman A, Williams G, and O'Callaghan C**. Ciliated air-liquid cultures as an aid to diagnostic testing of primary ciliary dyskinesia. *Chest* 138: 1441-1447, 2010.
10. **Horani A, Brody SL, Ferkol TW, Shoseyov D, Wasserman MG, Ta-shma A, Wilson KS, Bayly PV, Amirav I, Cohen-Cymberknoh M, Dutcher SK, Elpeleg O, and Kerem E**. CCDC65 mutation causes primary ciliary dyskinesia with normal ultrastructure and hyperkinetic cilia. *PLoS ONE* 8: e72299, 2013.
11. **Horani A, Ferkol TW, Shoseyov D, Wasserman MG, Oren YS, Kerem B, Amirav I, Cohen-Cymberknoh M, Dutcher SK, Brody SL, Elpeleg O, and Kerem E**. LRRC6 mutation causes primary ciliary dyskinesia with dynein arm defects. *PLoS ONE* 8: e59436, 2013.
12. **Horani A, Nath A, Wasserman MG, Huang T, and Brody SL**. Rho-Associated Protein Kinase Inhibition Enhances Airway Epithelial Basal-Cell Proliferation and Lentivirus Transduction. *Am J Respir Cell Mol Biol* 49: 341-347, 2013.
13. **Hornef N, Olbrich H, Horvath J, Zariwala MA, Fliegauf M, Loges NT, Wildhaber J, Noone PG, Kennedy M, Antonarakis SE, Blouin JL, Bartoloni L, Nusslein T, Ahrens P, Griese M, Kuhl H, Sudbrak R, Knowles MR, Reinhardt R, and Omran H**. DNAH5 Mutations Are a Common Cause of Primary Ciliary Dyskinesia With Outer Dynein Arm Defects. *Am J Respir Crit Care Med* 174: 120-126, 2006.
14. **Hussain S, Ji Z, Taylor AJ, DeGraff LM, George M, Tucker CJ, Chang CH, Li R, Bonner JC, and Garantziotis S**. Multiwalled Carbon Nanotube Functionalization with

High Molecular Weight Hyaluronan Significantly Reduces Pulmonary Injury. *ACS Nano* 10: 7675-7688, 2016.

15. **Jacobs JJ, Kieboom K, Marino S, DePinho RA, and van Lohuizen M**. The oncogene and Polycomb-group gene bmi-1 regulates cell proliferation and senescence through the ink4a locus. *Nature* 397: 164-168, 1999.

16. **Kesimer M, Kirkham S, Pickles RJ, Henderson AG, Alexis NE, Demaria G, Knight D, Thornton DJ, and Sheehan JK**. Tracheobronchial air-liquid interface cell culture: a model for innate mucosal defense of the upper airways? *Am J Physiol Lung Cell Mol Physiol* 296: L92-L100, 2009.

17. **Li Y, Yagi H, Onuoha EO, Damerla RR, Francis R, Furutani Y, Tariq M, King SM, Hendricks G, Cui C, Saydmohammed M, Lee DM, Zahid M, Sami I, Leatherbury L, Pazour GJ, Ware SM, Nakanishi T, Goldmuntz E, Tsang M, and Lo CW**. DNAH6 and Its Interactions with PCD Genes in Heterotaxy and Primary Ciliary Dyskinesia. *PLoS Genet* 12: e1005821, 2016.

18. **Liu X, Ory V, Chapman S, Yuan H, Albanese C, Kallakury B, Timofeeva OA, Nealon C, Dakic A, Simic V, Haddad BR, Rhim JS, Dritschilo A, Riegel A, McBride A, and Schlegel R**. ROCK inhibitor and feeder cells induce the conditional reprogramming of epithelial cells. *Am J Pathol* 180: 599-607, 2012.

19. **Livak KJ, and Schmittgen TD**. Analysis of relative gene expression data using real-time quantitative PCR and the 2(-Delta Delta C(T)) Method. *Methods* 25: 402-408, 2001.

20. **McKay TR, Camarasa MV, Iskender B, Ye JP, Bates N, Miller D, Fitzsimmons JC, Foxler D, Mee M, Sharp TV, Aplin J, Brison DR, and Kimber SJ**. Human feeder cell line for derivation and culture of hESc/hiPSc. *Stem Cell Res* 7: 154-162, 2011.

21. **Milyavsky M, Shats I, Erez N, Tang X, Senderovich S, Meerson A, Tabach Y, Goldfinger N, Ginsberg D, Harris CC, and Rotter V**. Prolonged culture of telomerase-immortalized human fibroblasts leads to a premalignant phenotype. *Cancer Res* 63: 7147-7157, 2003.

22. **Reynolds SD, Rios C, Wesolowska-Andersen A, Zhuang Y, Pinter M, Happoldt C, Hill CL, Lallier SW, Cosgrove GP, Solomon GM, Nichols DP, and Seibold MA**. Airway Progenitor Clone Formation is Enhanced by Y-27632-dependent Changes in the Transcriptome. *Am J Respir Cell Mol Biol* 2016.

23. **Rousseau K, Wickstrom C, Whitehouse DB, Carlstedt I, and Swallow DM**. New monoclonal antibodies to non-glycosylated domains of the secreted mucins MUC5B and MUC7. *Hybridoma and Hybridomics* 22: 293-299, 2003.

24. **Shoemark A, Dixon M, Beales PL, and Hogg CL**. Bardet Biedl Syndrome Motile Ciliary Phenotype. *Chest* 147: 764-770, 2015.

25. **Smith CM, Djakow J, Free RC, Djakow P, Lonnen R, Williams G, Pohunek P, Hirst RA, Easton AJ, Andrew PW, and O'Callaghan C**. ciliaFA: a research tool for automated, high-throughput measurement of ciliary beat frequency using freely available software. *Cilia* 1: 14, 2012.

26. **Smith CM, Kulkarni H, Radhakrishnan P, Rutman A, Bankart MJ, Williams G, Hirst RA, Easton AJ, Andrew PW, and O'Callaghan C**. Ciliary dyskinesia is an early feature of respiratory syncytial virus infection. *Eur Respir J* 43: 485-496, 2014.

27. **Suprynowicz FA, Upadhyay G, Krawczyk E, Kramer SC, Hebert JD, Liu X, Yuan H, Cheluvaraju C, Clapp PW, Boucher RC, Jr., Kamonjoh CM, Randell SH, and Schlegel R**. Conditionally reprogrammed cells represent a stem-like state of adult epithelial cells. *Proc Natl Acad Sci U S A* 109: 20035-20040, 2012.

28. **Torr E, Heath M, Mee M, Shaw D, Sharp TV, and Sayers I**. Expression of polycomb protein BMI-1 maintains the plasticity of basal bronchial epithelial cells. *Physiological Reports* 4: e12847, 2016.

29. **Tosoni K, Cassidy D, Kerr B, Land SC, and Mehta A**. Using Drugs to Probe the Variability of Trans-Epithelial Airway Resistance. *PLoS ONE* 11: e0149550, 2016.
30. **Wong AP, Bear CE, Chin S, Pasceri P, Thompson TO, Huan LJ, Ratjen F, Ellis J, and Rossant J**. Directed differentiation of human pluripotent stem cells into mature airway epithelia expressing functional CFTR protein. *Nat Biotechnol* 30: 876-882, 2012.
31. **Wong AP, and Rossant J**. Generation of Lung Epithelium from Pluripotent Stem Cells. *Curr Pathobiol Rep* 1: 137-145, 2013.
32. **Woollhead AM, Sivagnanasundaram J, Kalsi KK, Pucovsky V, Pellatt LJ, Scott JW, Mustard KJ, Hardie DG, and Baines DL**. Pharmacological activators of AMP-activated protein kinase have different effects on Na+ transport processes across human lung epithelial cells. *Br J Pharmacol* 151: 1204-1215, 2007.

AUTHOR CONTRIBUTIONS

M.M.M., A.S., R.A.H., J.M.D. and D.L.B. contributed to data collection. All authors contributed to study design, data analysis, interpretation of the data and critical revision of the final manuscript. All authors approved the final version of the manuscript.

GRANTS

This study was funded by the Great Ormond Street Hospital Children's Charity (GOSHCC), the Child Health Research Appeal Trust (CHRAT) and supported by the National Institute for Health Research Biomedical Research Centre at Great Ormond Street Hospital for Children NHS Foundation Trust and University College London.

DISCLOSURES

The authors declare no competing financial interests.

ADDITIONAL INFORMATION

Supplementary videos available.

FIGURE LEGENDS

Figure 1. BMI-1 maintains healthy cell morphology in 2D culture.

The morphology of (a) NHBE cells at passage 1 and (b) passage 3 was observed under light microscopy and compared to NHBE BMI-1 cells after passages (c) 11, (d) 17 and (e) 25. White arrows highlight elongated cells and black arrows highlight squamous cells. Scale bars are 100μm.

Figure 2. Karyotype analysis of NHBE-BMI-1 cells.

Karyotype of passage 23 NHBE-BMI-1 cells was undertaken by The Doctors Laboratory, London.

Figure 3. Elevated $p16^{Ink4a}$ precedes senescence and BMI-1 functions by inhibiting $p16^{Ink4a}$ and retains a normal cell doubling time.

(a) Western blot was used to assess levels of BMI-1 and $p16^{Ink4A}$ in serially passaged NHBE cells and BMI-1 transduced cells and (b) cell counting was used to determine the replication kinetics of NHBE and NHBE BMI-1 cells at varying passages. Growth curves are presented as percent of mean of day 1 cell count. Data are mean ± S.E.M. For each data point n=3 biological replicates.

Figure 4. BMI-1 cells retain their mucociliary differentiation capacity.

Extensively passaged BMI-1 transduced cells (passage 15) were differentiated on ALI and cilia beat frequency of (a) NHBE and (b) CFBE cells was determined using ciliaFA plugin(25) for ImageJ. Data are mean ± S.E.M; n= 4 independent ALI cultures, 5 fields videoed per culture. Immunostaining of NHBE-BMI-1 cells was used to show tight junction formation (occludin; c), mucin production (MUC5AC and MUC5B; d and e respectively), the presence of basal cells (p63+; f), widespread BMI-1 expression (BMI-1; g), and extensive ciliation (acetylated α-tubulin; h). TEM was used to determine cilia ultrastructure (i). Images are representative of 4 independent ALI cultures per marker. Scale bars for c-h are 50μm and 100nm for i.

Figure 5. BMI-1 cells form ALI cultures suitable for Ussing chamber studies.

Representative Ussing chamber traces and changes in short-circuit current (I_{sc}) in response to administration of amiloride (apical), forskolin (apical and basolateral) and GlyH-101 (apical) in primary and BMI-1 transduced (a and b) NHBE and (c and d) CFBE cells are shown. Data are mean ± S.E.M; n= at least 3 independent ALI cultures (see Table 4 for exact values).

Figure 6. DNAH5 knockdown recapitulates PCD phenotype.

(a) qRT-PCR was used to assess DNAH5 mRNA expression in NHBE-BMI-1 cells and NHBE BMI-1-transduced with lentivirus expressing either a scrambled or

DNAH5-targetting shRNA and grown in submerged 2D culture. **P<0.01; one-way ANOVA with Bonferroni's post-test used to assess significance. Data are mean ± S.E.M. (b) Immunostaining for DNAH5 and acetylated α-tubulin was used to assess the presence or absence of DNAH5 in the ciliary axoneme of shRNA transduced and untransduced NHBE BMI-1 cells differentiated at ALI. Presence of GFP fluorescence denotes cells transduced with the GFP-shRNA construct and so expressing the shRNA. Scale bars are 20μm. Images are representative of 4 independent ALI cultures per condition.

589 **TABLES**

590 **Table 1. Primary antibodies used in this study.**
591

Name	Supplier	Dilution WB/IF
Anit-MUC5AC	Life Technologies	NA/1:100
Anti-Acetylated α-tubulin	Sigma-Aldrich	NA/1:500
Anti-BMI-1	Life Technologies	1:200/1:100
Anti-GAPDH	Life Technologies	1:1000/1:500
Anti-MUC5B	Kind gift from Professor Dallas Swallow(23)	NA/neat
Anti-Occludin	Invitrogen, Life Technologies	NA/1:100
Anti-p16^{INK4}	Pharmingen, BD Biosciences	1:200/NA
Anti-p63	Invitrogen, Life Technologies	NA/1:100

592

593 **Table 2. Microtubule organisation of motile cilia.**
594

Microtubule Organisation	Frequency (%)
Normal 9+2	92.05
Central Pair Defect	0.66
Disarranged	3.31
Other Defect	3.97

595

596 **Table 3. Dynein arm presence in motile cilia.**
597

Dynein Arms	Frequency (%)
ODA and IDA Present	100.00
ODA Only	0.00
IDA Only	0.00
ODA and IDA Absent	0.00

598

599

Table 4. Trans-epithelial electrical resistance (TEER) measurements.

Name	Passage	TEER ($\Omega.cm^2$ ±S.E.M)	n
NHBE (AB053901)	P1	621.0 ± 33.2	5
NHBE (AB037501)	P1	331.1 ± 105.5	3
NHBE BMI-1	P13	1268.4 ± 78.4	4
CFBE	P2	1307.9 ± 36.6	5
CFBE BMI-1	P17	917.6 ± 165.3	6

Table 5. DNAH5 localisation.

	Is DNAH5 located in ciliary axoneme?	
shRNA Target	**Yes**	**No**
Untransduced	157	0
Scrambled	147	0
DNAH5	5	173

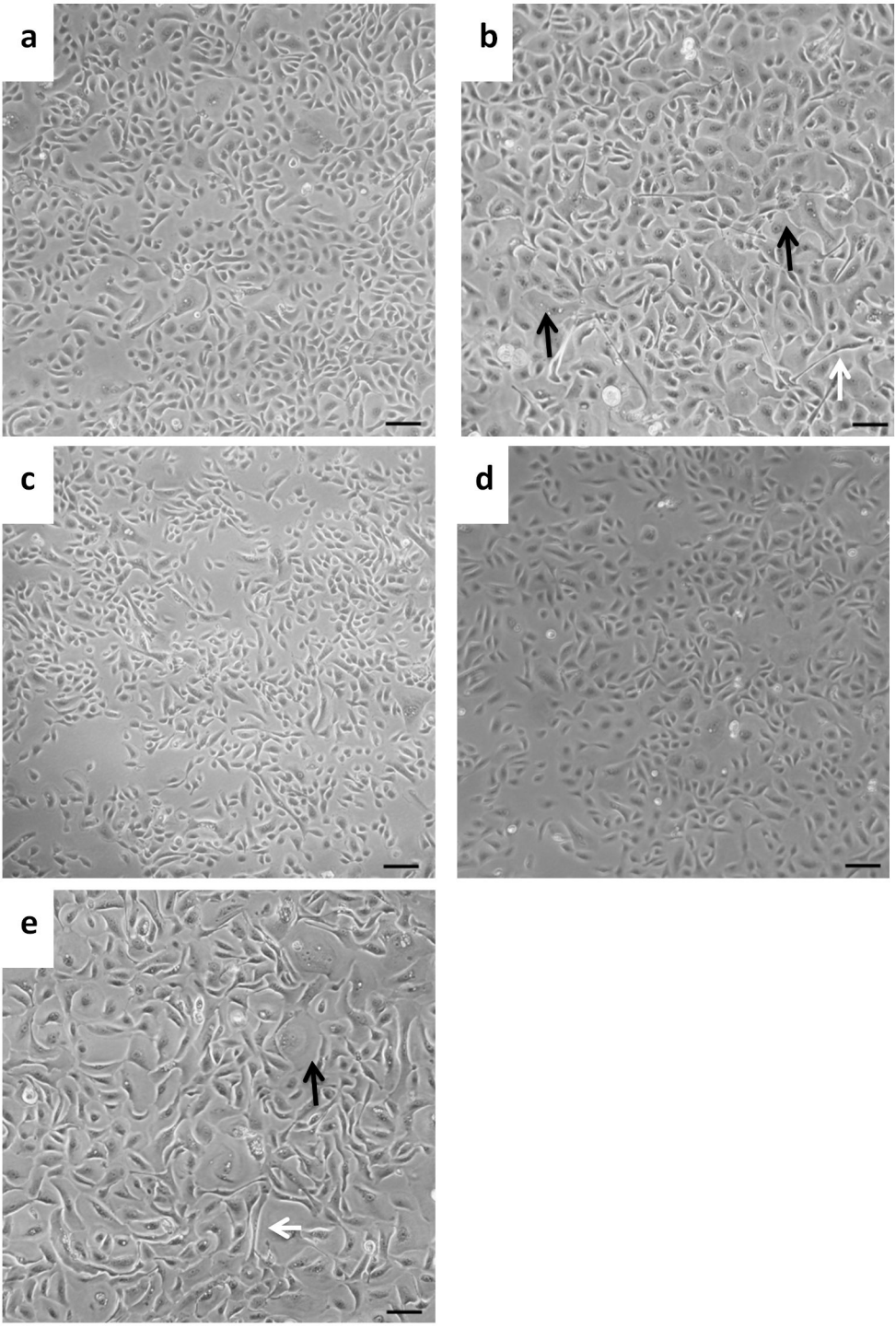

Figure 1

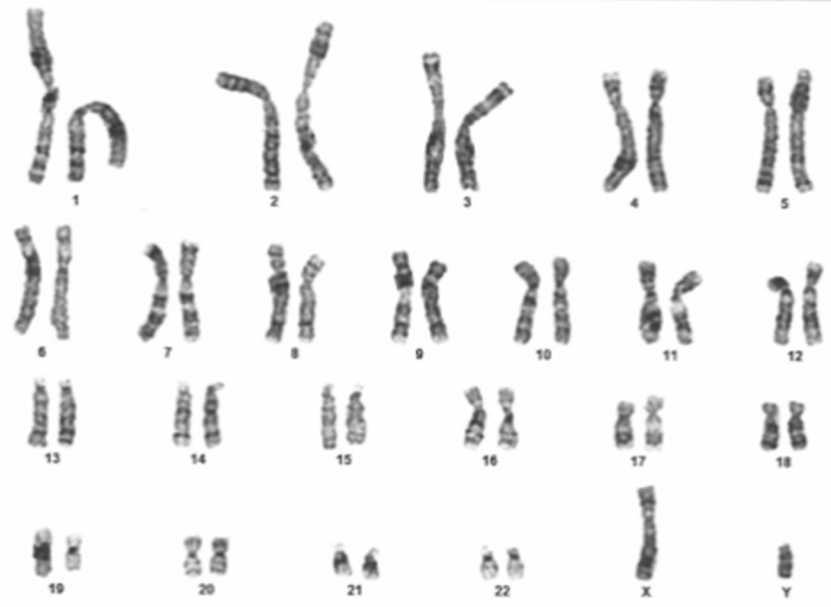

Figure 2

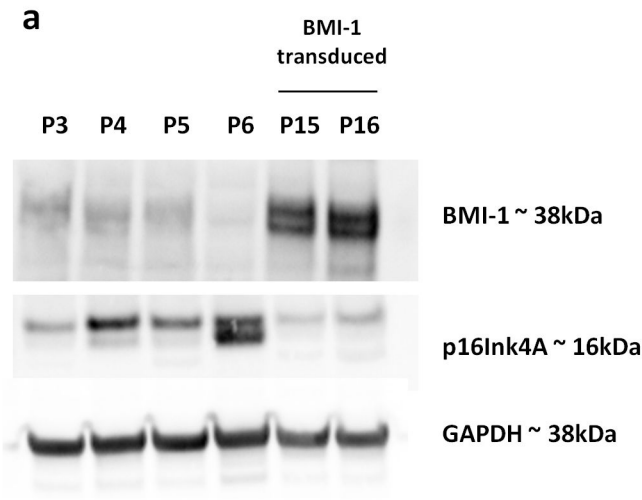
a
BMI-1
transduced
P3
P4
P5
P6
P15
P16
BMI-1 ~ 38kDa
p16Ink4A ~ 16kDa
GAPDH ~ 38kDa

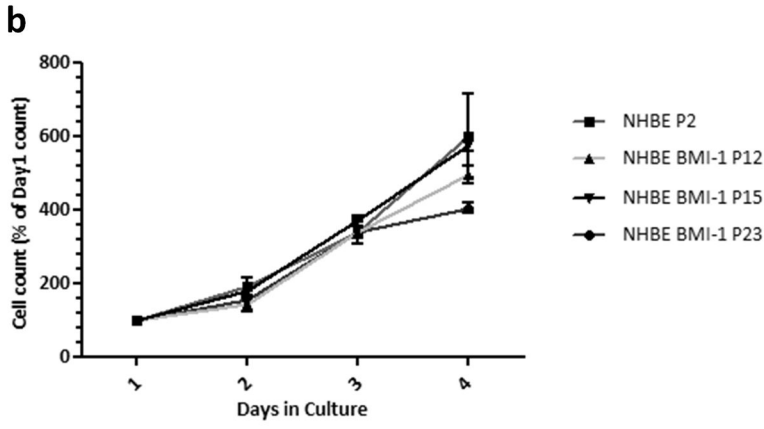
b
800
600
400
200
0
Cell count (% of Day1 count)
1
2
3
4
Days in Culture
NHBE P2
NHBE BMI-1 P12
NHBE BMI-1 P15
NHBE BMI-1 P23

Figure 3

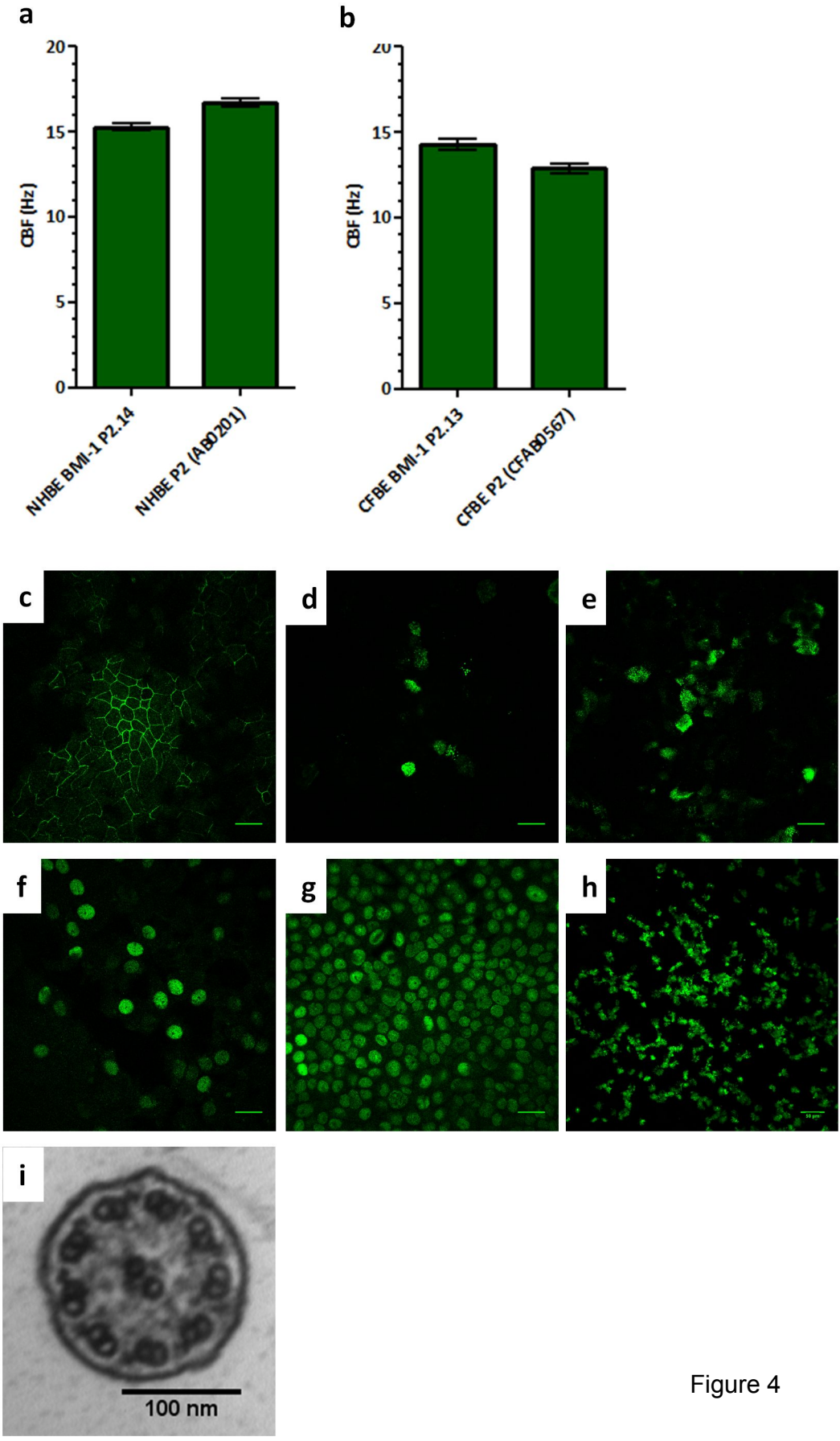
a
b
CBF (Hz)
20
15
10
5
0
NHBE BMI-1 P2.14
NHBE P2 (AB0201)
CFBE BMI-1 P2.13
CFBE P2 (CFAB0567)
c
d
e
f
g
h
i
100 nm

Figure 4

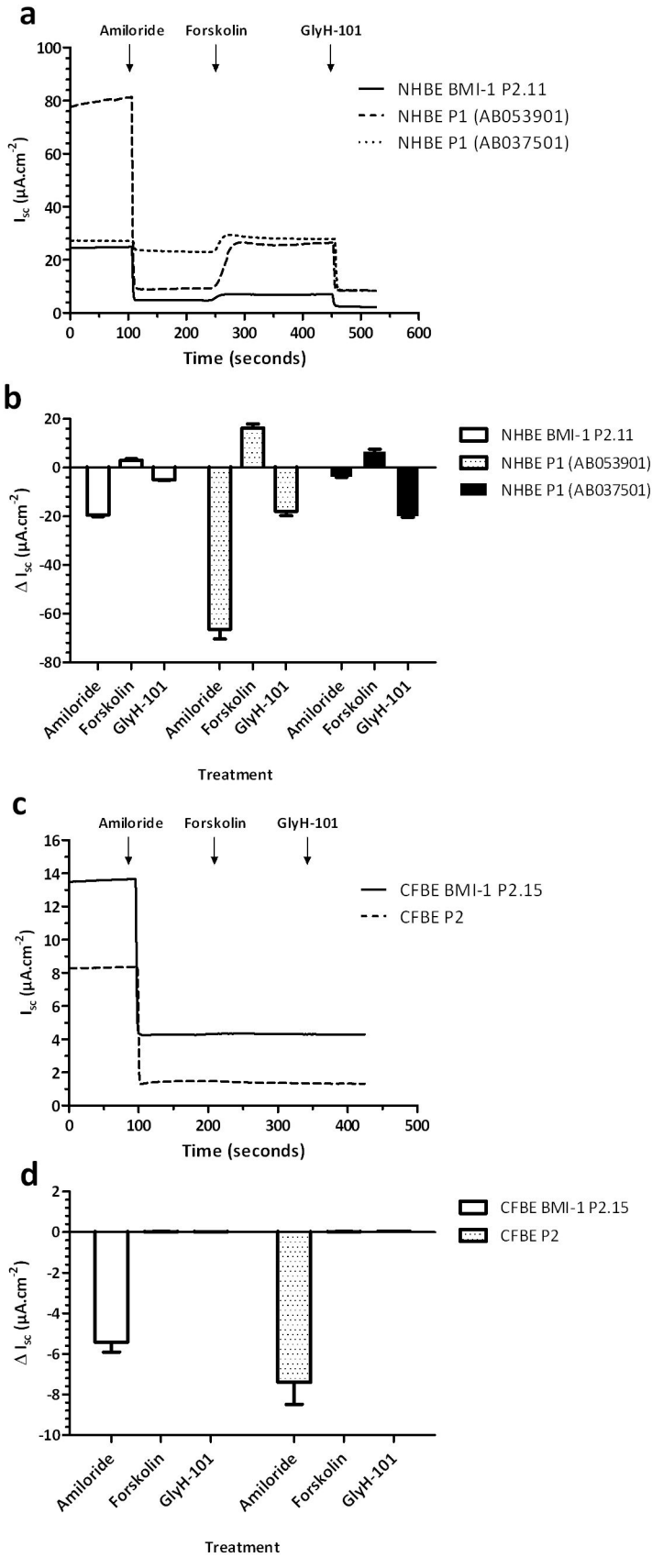
a
Amiloride
Forskolin
GlyH-101
NHBE BMI-1 P2.11
NHBE P1 (AB053901)
NHBE P1 (AB037501)
I_{sc} (µA.cm^{-2})
Time (seconds)
b
NHBE BMI-1 P2.11
NHBE P1 (AB053901)
NHBE P1 (AB037501)
Δ I_{sc} (µA.cm^{-2})
Amiloride
Forskolin
GlyH-101
Treatment
c
Amiloride
Forskolin
GlyH-101
CFBE BMI-1 P2.15
CFBE P2
I_{sc} (µA.cm^{-2})
Time (seconds)
d
CFBE BMI-1 P2.15
CFBE P2
Δ I_{sc} (µA.cm^{-2})
Amiloride
Forskolin
GlyH-101
Treatment

Figure 5

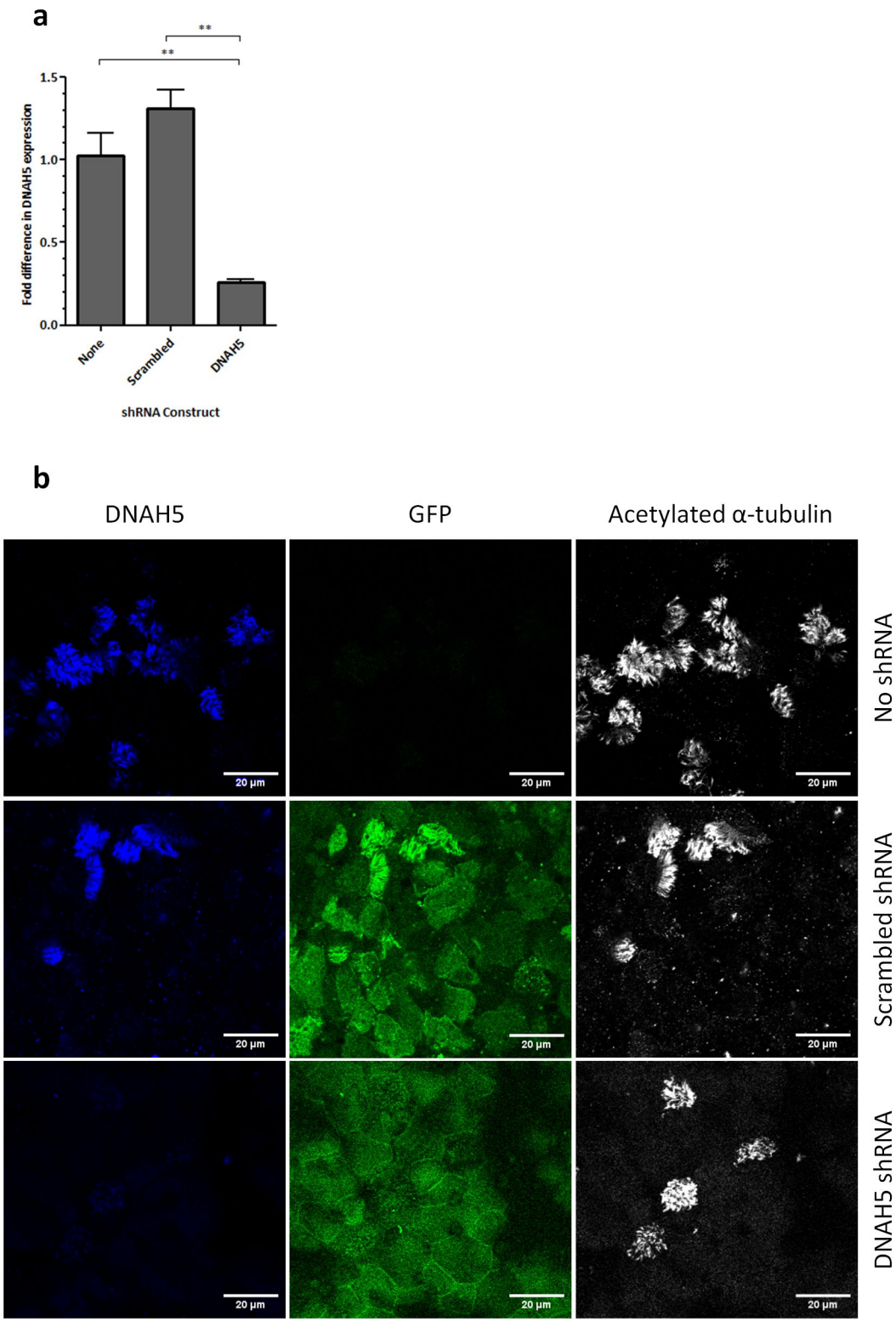
a
**
**
1.5
1.0
0.5
0.0
Fold difference in DNAH5 expression
None
Scrambled
DNAH5
shRNA Construct
b
DNAH5
GFP
Acetylated α-tubulin
No shRNA
Scrambled shRNA
DNAH5 shRNA
20 µm

Figure 6